applied sciences

MDPI

Article

Chestnut Burrs as Natural Source of Antimicrobial Bioactive Compounds: A Valorization of Agri-Food Waste

Alfonso Trezza [1,*,†], Roberta Barletta [1,†], Michela Geminiani [1,2], Luisa Frusciante [1], Tommaso Olmastroni [1], Filomena Sannio [3], Jean-Denis Docquier [3] and Annalisa Santucci [1,2,4]

[1] Department of Biotechnology, Chemistry & Pharmacy, University of Siena, Via A. Moro, 53100 Siena, Italy; r.barletta@student.unisi.it (R.B.); geminiani2@unisi.it (M.G.); luisa.frusciante@unisi.it (L.F.); tommaso.olmastroni@student.unisi.it (T.O.); annalisa.santucci@unisi.it (A.S.)
[2] SienabioACTIVE, Università di Siena, Via Aldo Moro, 53100 Siena, Italy
[3] Dipartimento di Biotecnologie Mediche, Università degli Studi di Siena, Viale Bracci 16, 53100 Siena, Italy; filomena.sannio@unisi.it (F.S.); jddocquier@unisi.it (J.-D.D.)
[4] ARTES 4.0, Viale Rinaldo Piaggio, 34, 56025 Pontedera, Italy
* Correspondence: alfonso.trezza2@unisi.it
† These authors contributed equally to this work.

Abstract: Currently, one-third of global food production, accounting for 1.3 billions tons, goes wasted due to major humanitarian and environmental challenges. In such a scenario, the circular bioeconomy model stands as an innovative solution by promoting sustainable production, utilizing agri-food waste, and converting non-renewable products into valuable resources. Here, the circular bioeconomy concept was applied on a previously obtained chestnut burr extract (agri-food waste) composed of gallic acid, quinic acid, protocatechuic acid, brevifolin carboxylic acid, and ellagic acid to evaluate its antimicrobial activity against four bacterial opportunistic pathogens (*Enterococcus faecalis*, *Staphylococcus aureus*, *Pseudomonas aeruginosa*, and *Escherichia coli*). Our results evidenced a modest but measurable antibacterial activity against *Enterococcus faecalis*, with a minimum inhibitory concentration (MIC) of 64 μg/mL. In silico studies allowed for identifying the potential molecular target, supporting the underlying antibacterial activity of the active principle and providing useful molecular findings regarding their interaction. In this study, we show a robust and comprehensive in vitro and in silico pipeline aimed at the identification of novel antibacterial scaffolds taking advantage of agri-food waste.

Keywords: chestnut burrs; circular bioeconomy; antimicrobial activity; *Enterococcus faecalis*; molecular modeling; docking simulations; molecular dynamics simulations; multiple sequence alignments; MIC

Citation: Trezza, A.; Barletta, R.; Geminiani, M.; Frusciante, L.; Olmastroni, T.; Sannio, F.; Docquier, J.-D.; Santucci, A. Chestnut Burrs as Natural Source of Antimicrobial Bioactive Compounds: A Valorization of Agri-Food Waste. *Appl. Sci.* **2024**, *14*, 6552. https://doi.org/10.3390/app14156552

Academic Editor: Ana M. L. Seca

Received: 9 July 2024
Revised: 22 July 2024
Accepted: 25 July 2024
Published: 26 July 2024

1. Introduction

Linear economics has underpinned the current growth in the world's population. Indeed, in the space of five decades, there has been an increase from 2.5 to 7.9 billion people, justified by the environmental capacity and resources [1]. Using natural resources and primary energy without considering alternatives is defined as linear economics. This approach is, however, the major contributor to the consumption and draining of natural sources, ultimately flowing into the severe environmental, economic, and social crisis the world is currently facing [1].

If linear economy depletes resources, circular economy instead implements environmental sustainability by encouraging resource reuse and recycling [2]. This perspective decreases both human impact and pollution derived from the waste [3].

A particularly noteworthy field of application for circular bioeconomy is scientific research, yielding a circular bioeconomy [4] where sustainable products are generated from biological wastes, mostly from food, industrial, and agricultural sources [3].

The exploitation of food wastes was for a long time as feed additives for animals [5]. Recently, other applications arose. For instance, biorefineries started exploiting wastes to produce natural renewable gas [6], and textile sector relied more on natural dyes, such as pomegranate seeds, for tissue staining [7].

Castanea sativa, known in Europe as sweet chestnut, is economically valuable for its nutrient-rich fruit, the chestnuts. Their abundance in carbohydrates, fibers, starch, fatty acids, minerals (potassium, phosphorous, calcium, and magnesium), and vitamins (B9, C, and E) [8–12] valorizes them in a Mediterranean diet [8,13] and for treating illnesses like diarrhea and cough [12].

The nuts are encased in a hard, spiky shell, and a typical glossy brown nut with a pointed tip is found within the husk. When cooked, chestnuts have a starchy and unique sweet flavor, and lower oil content compared to other nuts [14]. Interest in chestnut production is currently rising, especially in Spain, France, Brazil, the USA, and Switzerland, holding the lead in chestnut exportation rate (77.6%) [15]. Despite the relevance of *C. sativa* as a fruit crop, its bark in particular is used to extract tannins (vescalgin, castalin, and vescalin) and it accounts for 60% of the total amount of tannic substances [12].

Several studies have shown that chestnuts are rich in tannins in the bark and leaves; furthermore, chestnut byproducts (like the burr) represent a source of biomolecules with antioxidant, anticarcinogenic, and cardioprotective activity [11].

Burrs must be removed from the brush woods to ensure optimal growth of the tree (usually by burning them), causing damage in terms of time and financial resources. This practice is not only dangerous, but it also contributes to environmental pollution by releasing carbon dioxide.

From this perspective, the interest in a more sustainable chestnut exploitation process rose. Previous research already exploited chestnut shells to withhold pollutants from the environment, to produce energy through carbon combustion, and to generate active carbons as adsorbent molecules [16].

Another current application of agri-food wastes, mainly crop residues, sees them a source of various bioactive molecules. For instance, coffee husks are a fount of phenolic compounds, notoriously displaying antioxidant activity [1]. In the chestnut burrs of *C. sativa* particularly abundant is ellagic acid with antioxidant properties, as well as an antimicrobial effect against *Helicobacter pylori* [17]. *Enterococcus faecalis* is a Gram-positive bacterium able to cause hospital-acquired infections (HAI), urinary tract infections (UTIs), bacteremia, valve endocarditis, and wound infections [18,19]. Currently, endocarditis, bacteremia, and UTI treatments are represented by combination therapy, consisting of the coadministration of cell wall-active agents, such as β-lactams, and aminoglycosides [19]. However, *E. faecalis* presents with a decreased susceptibility to penicillin and ampicillin [20], and intrinsic low-level resistance to aminoglycosides, leading to worrying and growing antimicrobial resistance levels [21].

In this setting, an innovative in vitro and in silico pipeline was developed to investigate the antimicrobial activity of a previously characterized chestnut burr biomass extract [22].

In vitro MIC assays showed significant antimicrobial activity against Gram-positive *E. faecalis* but not against other tested strains (*Staphylococcus aureus*, *Escherichia coli*, and *Pseudomonas aeruginosa*).

In silico analysis identified potential bioactive compounds and *E. faecalis* targets, revealing pharmacodynamic features through molecular dynamic simulations.

Overall, this approach focuses on potentially innovative applications within the circular bioeconomy, utilizing natural waste as a source of antimicrobial bioactive compounds.

2. Materials and Methods

2.1. Preparation of C. sativa Burrs (CSB) Extract

C. sativa burrs extract was prepared as previously described [22]. The spiny burrs of Castanea *sativa* (Mill.), certified under the PGI (Protected Geographical Indication) Castagna del Monte Amiata (Reg. CEE n. 2081/92), were obtained from Tuscany, a notable

chestnut-producing region in Italy. The burrs were meticulously cleaned and air-dried at room temperature until they reached a stable weight. Subsequently, they were ground into a fine powder and stored in sealed, dark plastic bags at −80 °C to be preserved until extraction. The extraction process involved immersing 330 g of the powdered burrs in 1 L of water and treating the mixture with 20 kHz ultrasonic waves for three hours at room temperature. The resulting aqueous extract, referred to as CSB, was then freeze-dried using a lyophilizer (Lyovapor L-200, Bhuchi, India) and kept at −32 °C for further experiments.

2.2. In Vitro Antibacterial Susceptibility Testing

Enterococcus faecalis ATCC 29212, *Staphylococcus aureus* ATCC 25392, *Escherichia coli* ATCC 25922, and *Pseudomonas aeruginosa* ATCC 27853 were obtained from the American Type Culture Collection (Manassas, VA, USA) and conserved at –80 °C in Brain–Heart Infusion (BHI) medium supplemented with 30% glycerol. All bacteria were routinely grown aerobically on Mueller–Hinton agar plates incubated at 37 °C for 18–24 h. The extracts were resuspended in DMSO at a final concentration of 50 mg/mL and subsequently diluted in the culture medium. Minimum inhibitory concentrations (MICs) of the extracts were determined in triplicate in Mueller–Hinton medium using the microdilution broth method and a bacterial inoculum of 5×10^4 CFU/well, as recommended by the Clinical Laboratory Standards Institute (CLSI). Briefly, serial twofold dilutions of the extract were prepared extemporaneously in a 96-well plate (final volume in well, 90 µL), prior to the addition (10 µL) of the bacterial suspension containing 5×10^6 CFU/mL. Final DMSO concentration in the well did not exceed 1%. Growth controls were carried out in parallel using up to 1% DMSO in the well (no growth inhibition could be observed with any of the tested organism). MICs were recorded after 18 h of incubation at 35 ± 2 °C. Vancomycin and colistin (tested at concentrations ranging 32-0.015 µg/mL) were used as antibiotic controls for *E. faecalis* and *S. aureus*, or *E. coli* and *P. aeruginosa*, respectively.

2.3. In Silico Methods

2.3.1. Sequence Resources and Multiple Sequence Alignment

The *E. faecalis* ATCC 29212 strain protein primary structures (197 sequences) were downloaded from the NCBI genome database (NCBI RefSeq assembly: GCF_000742975.1) in FASTA format, while the *P. aeruginosa* (110.903 sequences), *S. aureus* (108.451 sequences), and *E. coli* (543.617 sequences) protein primary structures were retrieved and extracted from the entire "Non-redundant protein sequences (nr)" database, which contains nearly all protein sequences available at NCBI [23]. The Blastp tool performed a multiple sequence alignment (MSA) between the *E. faecalis* sequences and the *P. aerugimosa*, *S. aureus*, and *E. coli* sequences (collected in a unique FASTA file containing 762.971 sequences) using BLOSUM 62 matrix, a word size of 6, E-value of 0.01, adding the flag -sorthits 3 and -sorthsps 0 to sort the MSA output for identity and E-value, respectively; all other parameters were set by default [23]. MSA results provided an output of 150.305.287 sequence alignments; thus, a python script written in-house extracted all *E. faecalis* sequences (38 sequences), which did not show any identity/similarity with the sequences of the other bacteria strains (with a similarity/identity value less than 20%). The 38 sequences of *E. faecalis* were analyzed in the UniProt database [24] and all sequences annotated as "obsolete" were discarded. From the UniProt searches, only one sequence was obtained: "endocarditis and biofilm-associated pilus tip protein EbpA" (NCBI Reference Sequence: WP_148304834.1).

2.3.2. Molecular Modeling and Structural Optimization

The von Willebrand factor type A (vWA) structural domain 3D structure of the *Eca* endocarditis and biofilm-associated pilus tip protein EbpA was generated by AlpfaFold [25] using the NCBI Reference Sequence WP_148304834.1 as a target. AlphaFold predicted 5 different 3D structures using different weights and ranked them from best to worst by their mean pLDDT; the uncertainty metric ranges between 0 and 100, where 0 means high certainty and 100 means high uncertainty (lower is better). We selected the first model as

the best 3D structure generated by AlphaFold, showing an uncertainty value of 2.81% with a mean pLDDT of 85.75, suggesting high confidence of the whole 3D structure. The Mg^{2+} ion was added to the structure, through structural superimposition, using as template the "Crystal structure of pilus adhesin, SpaC from Lactobacillus rhamnosus GG—open conformation" of *Lacticaseibacillus rhamnosus* (PDB code: 6M3Y) [26].

2.3.3. In Silico Docking and Molecular Dynamics Simulations

The 3D structure was optimized using PyMOD3.0 [27] with MODELLER 10.5 and validated through PROCHECK [28] to prevent errors during the molecular dynamic (MD) simulations. The parameters of the force field were assigned by CHARMM-GUI platforms [29] and GROMACS 2019.3 [30] carried out the MD run as suggested in a previous works [31,32], where the structure was enclosed, in a triclinic box filled with TIP3P water molecules and counter ions to neutralize the net charge of the system. The system was minimized 5.000 steps using steepest descent algorithm to a minimum energy with forces less than 100 kJ/mol/nm [33]. A cMD simulation was integrated each 2 fs, while a V-rescale thermostat and Nose–Hoover barostat led the temperature and pressure at 300 K and 1 atm, respectively. MD run was of 150 ns.

The "gmx cluster" function extracted the frame most representative of the MD run and it was used as target for the docking simulation of compounds extracted by the chestnut burrs. The 3D structures of gallic acid, quinic acid, protocatechuic acid, brevifolin acid, and ellagic acid were retrieved from the PubChem database [34] (with compound CID: 370, 6508, 72, 9838995, and 5281855, respectively) and downloaded in sdf format. A box with dimensions of 20 × 20 × 20 Å was created around the sensing region of the target using DockingPie2.0 [35] implemented in PyMOL 3.0 using Autodock/Vina as a docking tool [36,37]. Docking simulation was set with exhaustiveness of 32, selecting only the binding poses with RMSD lower of 2 Å with a binding free energy value of at least −7 Kcal/mol. All other parameters were used as default. P.L.I.P. Tool [38,39] provided the interaction network. The alignment of sequences were performed with ClustalW [40]. The best complexes were selected and subjected to cMD run, with the same protocols previously described.

All MD analyses were explored with GROMACS 2019.3 packages. GRACE generated the MD graphs and PyMOL 3.0 was used as a molecular graphic interface and produced the biological system pictures. All simulations and analyses were computed using a workstation with CPU AMD Ryzen Threadripper PRO 5965WX 24 Core (4.5 GHz, 140 MB CACHE), DDR4 Kingston 3200 MHz 128 GB RAM, Nvidia GeForce RTX4090 24 GB graphic card, and SSD NVME M.2 of 2 TB + 2x HDD S-ATA3 of 14 TB as storage partition with OS Linux Mint 21.1.

3. Results

3.1. Extract Susceptibility in Bacterial Strains

Results from the MIC assay are reported in Table 1. The MIC value measured with *E. faecalis* ATCC 29212 was 64 µg/mL, thereby proving an antimicrobial activity, although modest, of the chestnut extract against this strain. No such activity was confirmed for the other strains. Indeed, in *S. aureus* ATCC 25392, the MIC value was 512 µg/mL. In *E. coli* strain CCUG^{T} and *P. aeruginosa* ATCC 27853, the observed MIC values were >512 µg/mL. The MIC values of such control antibiotics are reported in Table 1.

Table 1. Determination of MIC values of the chestnut burrs extract (CBE) on *E. faecalis*, *S. aureus*, *E. coli*, and *P. aeruginosa*. The MIC values of the reference antibiotics (vancomycin or colistin, showing the expected activity on either Gram-positive or Gram-negative organisms, respectively) are also indicated.

Organism	MIC (μg/mL)		
	CBE	Vancomycin	Colistin
E. faecalis	64	2	>32
S. aureus	512	1	>32
E. coli	>512	>32	0.25
P. aeruginosa	>512	>32	0.5

3.2. Multiple Sequence Alignments

In silico results showed a susceptibility of the *E. faecalis* strain against the *C. sativa* extract (gallic acid, quinic acid, protocatechuic acid, brevifolin acid, and ellagic acid), differently, the other strains (*P. aeruginosa*, *S. aureus*, and *E. coli*) did not exhibit any vulnerability after the treatment with the extract.

Based on the evidence that our extract was active only on the *E. faecalis* strain, we detected the potential *E. faecalis* targets, involved in the interaction with our compounds, by performing an MSA of the entire *E. faecalis* protein pool against the entire "Non-redundant protein sequences (nr)" database of the *P. aeruginosa*, *S. aureus*, and *E. coli* strains to identify the *E. faecalis* non-homologue sequences aligned with the sequences of the other strains.

A Python script written in-house analyzed 150.305.287 alignment of sequences and provided 38 *E. faecalis* protein sequences that showed appropriate coverage and a similarity/identity value of less than 20% (non-homologous sequences). The sequences were explored on the UniProt database and all sequences that were annotated as "obsolete" were discarded; our analysis identified the endocarditis and biofilm-associated pilus tip protein EbpA (EbpA) as the only *E. faecalis* non-homologue sequence.

3.3. Molecular Modeling and Docking Simulations

AlphaFold generated and optimized the target 3D structure, while molecular modeling solved potential structural gaps and steric clashes. Gallic acid, quinic acid, protocatechuic acid, and brevifolin acid ellagic acid were tested against the target through in silico virtual screening. Two different strategies were applied to select the best complexes: (i) selecting only the compounds that showed a binding free energy (docking score) lower than −7 kcal/mol and (ii) the ability of the compound to trigger strong interactions with target *consensus* binding residues.

The docking results showed that the best complexes were EbpA/brevifolin and EbpA/ellagic acid providing a binding free energy of −7.8 kcal/mol and −7.3 kcal/mol, respectively. Interaction network analyses showed that the brevifolin and ellagic acid docked in a similar binding pose and formed a polar and hydrophobic interaction network within the target binding pocket (Figure 1A,B). Furthermore, docking results revealed the ability only of the ellagic acid to trigger H-bonds with target key residues, Asp-326 and Asp-429, both involved in the coordination of Mg^{2+} metal cofactor. Our results suggested the ability of the compounds to spontaneously bind on *E. faecalis* EbpA by forming a significant interaction network. The best two complexes were further explored in silico to define in detail the pharmacodynamic features of compounds against the target.

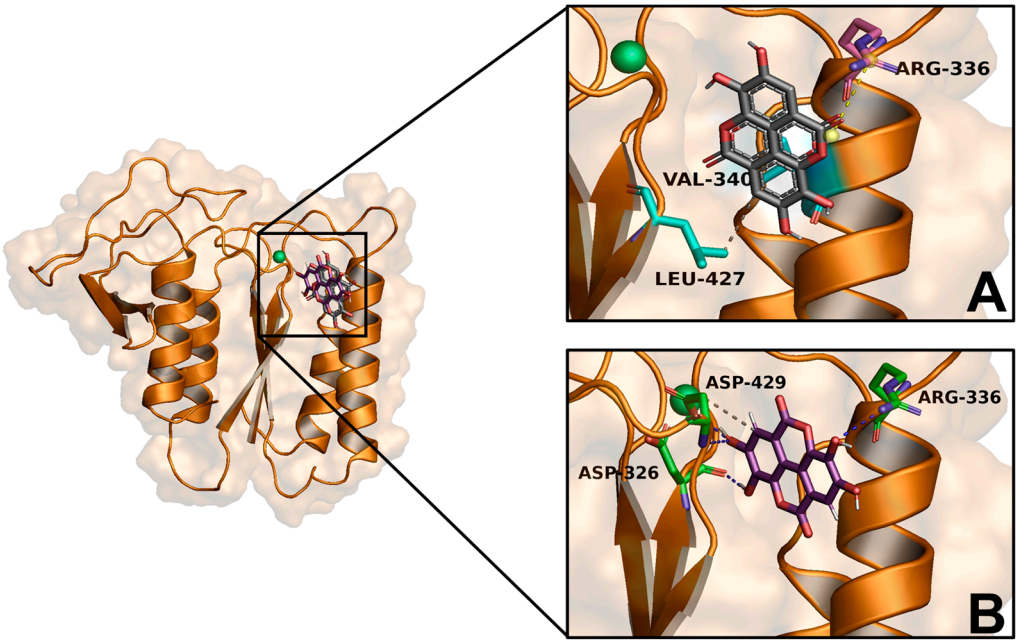

Figure 1. Overview of the docked pose of ellagic acid and brevifolin acid in complex with EbpA. EbpA3D structure is depicted in transparency orange cartoon/surface, while the magnesium ion was reported as a green sphere. Interaction network of (**A**) brevifolin (in gray) acid and (**B**) ellagic acid (in purple) in complex with EbpA after the docking simulation. The binding residues forming hydrophobic interactions (grey dashed lines), hydrogen bonds (blue dashed lines), and salt bridges (yellow dashed lines) are shown as cyan, green, and pink sticks, respectively.

3.4. cMD: EbpA/Ellagic Acid Complex (RMSD and Total Interaction Energy)

The target/compound interaction was dissected by analyzing structural and energy features performing cMDs for each complex and free state EbpA. To define the stability of the binding pose of compounds within the target binding pocket, the distance between the center of mass of the ligand and the center of mass of the binding pocket was evaluated. Ellagic acid showed a stable distance trend, suggesting high binding pose stability; surprisingly, brevifolin left the target binding pocket in the first frames of the MD run (Supplementary Materials Figure S1), likely due to the different interactions of the starting docking pose; thus, the EbpA/brevifolin complex was not considered for further MD analysis.

The target backbone structural integrity was assessed by evaluating the RMSD values for the EbpA/ellagic acid complex and free state EbpA. RMSD analyses suggested good structural stability, showing a stable RMSD trend of 0.15 Å and 0.2 Å for the complex and the free state, respectively. However, the EbpA/ellagic acid complex RMSD trend showed a higher RMSD value (moreover in the last frames of the MD run) than free state EbpA, exhibiting a significant increase of RMSD value until 0.25 Å. The binding pose of the compound within the target binding pocket did not significantly show fluctuations during the MD run, providing a very stable RMSD range between 0.03 Å and 0.05 Å, confirming the high stability and reliability of the selected starting docking pose (Figure 2). To strengthen the impact of the docking and cMD simulation, the target/compound interaction energy was evaluated. From energy analyses, we noticed that our compound was able to spontaneously bind on the target with a total interaction energy of -38.1 ± 3.8 kcal/mol (Figure S2).

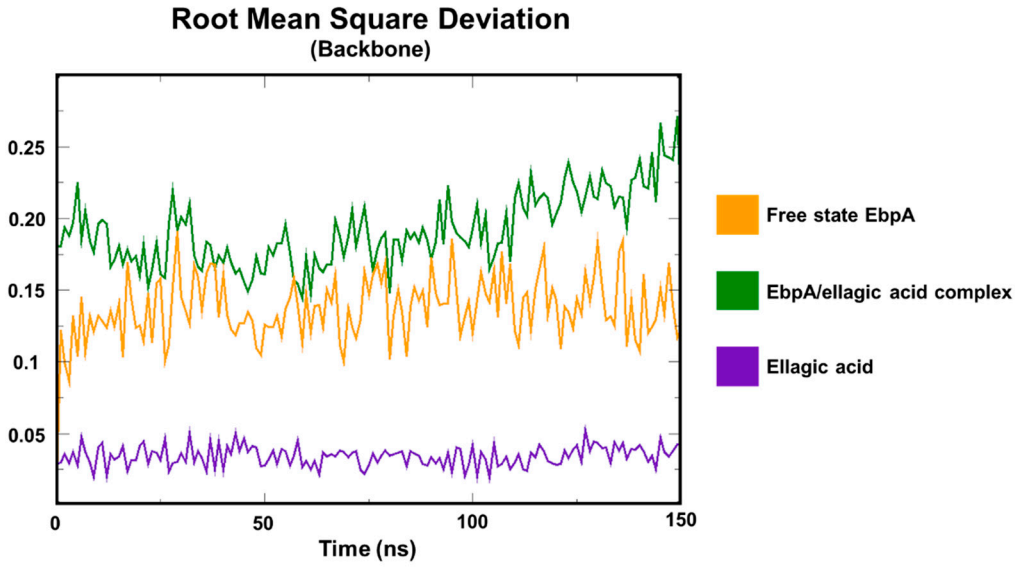

Figure 2. RMSD trends. RMSD profiles were evaluated for free state and EbpA/ellagic acid backbone along the entire MD run.

3.5. cMD: EbpA/Ellagic Acid Complex Interaction Network and Occupancy Analysis

To further explore the potential inhibitory activity of the ellagic acid in complex with the target, the dynamics interaction network was deeply explored during the MD run. The Prolif tool was used to detect both all target/compound interaction types and the occupancy of each interaction identified. Interestingly, interaction network analyses provided several polar and non-polar interactions (Figure 3A) and very high occupancy values. In detail, ellagic acid triggered van der Waals contacts with Arg-336 (50% of occupancy) and Leu-427 (81.25% of occupancy); hydrophobic interactions with Met-331 (87.5% of occupancy), Asp-339 (56.25% of occupancy), and Val-340 (100% of occupancy); and hydrogen bonds with Asp-326 (43.75% of occupancy) and Asp-429 (87.5% of occupancy) (Figure 3B).

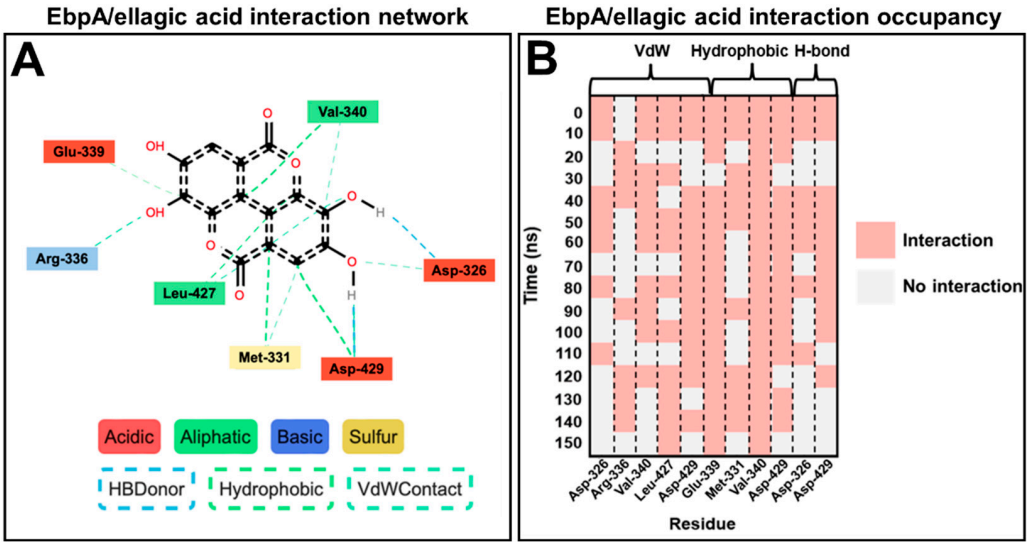

Figure 3. Interaction network and MD interaction network occupancy. (**A**) 2D interaction network among target binding residues and ellagic acid (in black). The involved target residues are labelled as acidic (in red), aliphatic (in green), basic (in blue), and sulfur (in yellow). The hydrogen bonds, hydrophobic interactions, and Wan der Waals contacts are represented as light blue, green, and cyan dashed lines, respectively. (**B**) EbpA/ellagic acid MD interaction network occupancy. The binding residues and the molecular dynamics run time are reported on the x- and y-axis, respectively. The target

residues are grouped on the interaction type (VdW, hydrophobic and H-bonds). The occupancy indicates the presence of each interaction over the simulation time; the pink color indicates the interaction presence; grey color means no interaction.

The role of the binding residues involved in the interaction with the ellagic acid was further explored by applying an evolutionary approach to define the conservation of residues along the protein evolution. The BLASTp tool performed MSA between the EbpA primary structure and the entire "non-redundant protein sequences (nr)" database excluding the *E. faecalis* organism and the Skylign tool analyzed the MSA results. Surprisingly, from the MSA analyses, we noted that Asp-326, Met-331, and Asp-429 showed a full conservation exhibiting a Shannon's entropy of 1 (Figure S3).

4. Discussion

Nowadays, climate change has been recognized as a major global challenge. Some strategies, such as the advancement of bioeconomy and sustainable forest management have proven to be crucial in tackling this global problem. The primary economic sector, driven by biological and "Protected Geographical Indication" products, has been acquiring a growing economic/social/environmental importance as shown by the latest trends in national agricultural metrics [2].

A plethora of natural sources, such as plants and microorganisms, stand as alternative sources of bioproducts with medicinal potential. Indeed, from these organisms, innovative compounds with biological activity can be isolated. For centuries, natural compounds have been harnessed in Chinese medicine as modulators of various signaling pathways like cell proliferation, angiogenesis, survival, and apoptosis, exhibiting different biological activities like antioxidant and anti-inflammatory properties.

Chestnut (*Castanea sativa*) cultivation has been deep sitting in Italy, particularly within its hilly and mountainous regions. As of 2017, Italy emerged as the leading producer of chestnuts in the European Union, contributing 52,356 tons, representing 38% of the total chestnut production in the EU (FAOSTAT, Food and Agriculture Organization of the United States). Nevertheless, this trend has been threatened in recent decades due to diseases such as chestnut blight and chestnut gall wasp, alongside the progressive depopulation of rocky areas.

In response to these issues, there has been a drive towards novel approaches to utilize various parts of the chestnut plant, such as the burrs, accounting for 10–15% of the total weight of chestnuts and currently employed in fuel and fermentable sugar production [3]. Burrs also exhibit multiple biological activities (anti-inflammatory, antioxidant, and antimicrobial) [11], hence the interest in investigating their potential as green sources of bioactive compounds.

Recently, the rising levels of resistant bacteria result in a threat for public health. This condition raised growing interest in antimicrobial resistance (AMR) and several approaches to investigate the antimicrobial activity of bio-compounds extracted from natural wastes have successfully been applied. Olive mill waste and artichoke bracts were both found to be successfully active against foodborne pathogens [41,42].

The current literature body already suggests antimicrobial activity from chestnut burrs, against *S. aureus*, *E. faecalis*, *Listeria monocytogenes* [43], and *E. coli* [44], confirmed by in vitro antimicrobial susceptibility assays. Here, however, an integrated in vitro and in silico workflow was adopted. After evaluating the antimicrobial activity of our chestnut burr extract [22,45] on different bacterial strains, a potential bacterial target of extract compounds (gallic acid, quinic acid, protocatechuic acid, brevifolin acid, and ellagic acid) was sought.

Firstly, an in vitro MIC assay was performed on both Gram-positive (*E. faecalis* and *S. aureus*) and Gram-negative (*E. coli* and *P. aeruginosa*) bacterial strains, yielding a measurable antimicrobial activity on *E. faecalis* (MIC = 64 μg/mL) only. Hence, the antimicrobial activity of the extract could be attributable to the interaction of the bioactive compound(s) with a specific target solely present in *E. faecalis* and not in all the other strains.

Multiple sequence alignment of *E. faecalis* proteins identified "endocarditis and biofilm-associated pilus tip protein EbpA" after removing homologous and obsolete sequences. The 3D structure of EbpA was created with AlphaFold. Subsequent computational screening revealed ellagic acid and brevifolin acid as potential antimicrobial compounds, with ellagic acid being the most abundant in the extract, but molecular dynamics simulations showed a stable binding only between ellagic acid binding and EbpA, while brevifolin rapidly dissociated. Network interaction analyses confirmed strong binding between ellagic acid and EbpA.

Asp-326 and Asp-429, involved in the coordination with the Mg^{2+} cofactor, were found as conserved residues by evolutionary analyses, further confirming docking and MD simulation. Furthermore, Met-331 binding residue was found located closely to the metal cofactor site, which is fully conserved. Despite the current absence of data on its functional/structural role in EbpA, our computational study implemented with the evolution approach would however propose it as a key residue for EbpA.

5. Conclusions

Our research was framed in a circular bioeconomy optics, where natural waste became a source of bioactive compounds targeting molecules involved in disease onset (bacterial infections, in this case). Through a combined in vitro and in silico approach, it was possible to discover novel bioactive material and their targets, simultaneously boosting the process's efficiency and cost-effectiveness.

In vitro and in silico data suggested an antimicrobial activity of *C. sativa* burrs extract against *E. faecalis.* Indeed, in vitro MIC assays showed bacterial susceptibility to the extract, with a MIC value of 64 ug/mL. Then, the unique bacterial target was pointed out, and the ligand–target interaction was investigated with docking and MD simulations. Those combined findings on the possible interaction between ellagic acid in the extract and the target protein EbpA of *E. faecalis* prepared the ground for further experimental validation with in vitro binding assays.

Overall, this initial step of target discovery proposes a green and sustainable scientific pipeline to investigate the biological activity of compounds extracted from agro-forest wastes. This would noticeably reduce time, costs, and chemical waste, thus addressing the detrimental impact of pollutants on the planet. Ultimately, if supported by further research, wastes would be employed as a cost-effective antimicrobial material for various applications (agro-food or chemical industry, healthcare, etc.).

Supplementary Materials: The following supporting information can be downloaded at: https://www.mdpi.com/article/10.3390/app14156552/s1, Figure S1: Minimum distance profiles; Figure S2: Interaction energy trends of ellagic acid bound within target binding pocket; Figure S3: LOGO representation of MSA of the EbpA primary structure against the "bacteria" database in BLASTp.

Author Contributions: Conceptualization, A.T.; methodology, A.T., R.B. and J.-D.D.; software, A.T.; validation, A.T., A.S. and J.-D.D.; formal analysis, A.T. and J.-D.D.; investigation, A.T., R.B., F.S. and J.-D.D.; resources, A.S.; data curation, A.T., J.-D.D. and A.S.; writing—original draft preparation, A.T., R.B., J.-D.D. and A.S.; writing—review and editing, A.T., R.B., M.G., L.F., J.-D.D. and A.S.; visualization, A.T., R.B., M.G., L.F., T.O., J.-D.D. and A.S.; supervision, A.S.; project administration, A.S.; funding acquisition, A.S. All authors have read and agreed to the published version of the manuscript.

Funding: This research received no external funding.

Institutional Review Board Statement: Not applicable.

Informed Consent Statement: Not applicable.

Data Availability Statement: The original contributions presented in the study are included in the article/supplementary material, further inquiries can be directed to the corresponding author/s.

Acknowledgments: The authors thank PRIN: PROGETTI DI RICERCA DI RILEVANTE INTERESSE NAZIONALE—Bando 2022 Prot. 2022LW54KC; PRIN: PROGETTI DI RICERCA DI RILEVANTE INTERESSE NAZIONALE—Bando 2022 PNRR Prot. P2022RYR5W; CHEBAPACK Programma di

Sviluppo Rurale 2014–2020 Regione Toscana; PSR 2014–2020 Regione Toscana OPENRICCIO; F-Cur funds to M.G.; UE—FSE REACT-EU, PON Ricerca e Innovazione 2014–2020; Progetto ERICA ARTES 4.0, E87G23000100001 Agenzia Coesione Territoriale.

Conflicts of Interest: The authors declare no conflicts of interest.

References

1. Bongaarts, J. Human population growth and the demographic transition. *Philos. Trans. R. Soc. Lond. B Biol. Sci.* **2009**, *364*, 2985–2990. [CrossRef]
2. Di Vaio, A.; Hasan, S.; Palladino, R.; Hassan, R. The transition towards circular economy and waste within accounting and accountability models: A systematic literature review and conceptual framework. *Environ. Dev. Sustain.* **2023**, *25*, 734. [CrossRef]
3. Venkatesh, G.; Se, V.G. Circular Bio-economy-Paradigm for the Future: Systematic Review of Scientific Journal Publications from 2015 to 2021. *Circ. Econ. Sustain.* **2022**, *2*, 231–279. [CrossRef]
4. Ghangrekar, M.M.; Das, S.; Das, S. Microbial Electrochemical Technologies for CO_2 Sequestration. In *Biomass, Biofuels, Biochemicals. Circular Bioeconomy—Current Status and Future Outlook*; Elsevier: Amsterdam, The Netherlands, 2021; pp. 413–443. [CrossRef]
5. Zhu, Y.; Luan, Y.; Zhao, Y.; Liu, J.; Duan, Z.; Ruan, R. Current Technologies and Uses for Fruit and Vegetable Wastes in a Sustainable System: A Review. *Foods* **2023**, *12*, 1949. [CrossRef] [PubMed]
6. Pham, T.P.T.; Kaushik, R.; Parshetti, G.K.; Mahmood, R.; Balasubramanian, R. Food waste-to-energy conversion technologies: Current status and future directions. *Waste Manag.* **2015**, *38*, 399–408. [CrossRef]
7. Popescu, V.; Blaga, A.C.; Pruneanu, M.; Cristian, I.N.; Pîslaru, M.; Popescu, A.; Rotaru, V.; Crețescu, I.; Cașcaval, D. Green Chemistry in the Extraction of Natural Dyes from Colored Food Waste, for Dyeing Protein Textile Materials. *Polymers* **2021**, *13*, 3867. [CrossRef]
8. Silva, V.; Falco, V.; Dias, M.I.; Barros, L.; Silva, A.; Capita, R.; Alonso-Calleja, C.; Amaral, J.S.; Igrejas, G.; Ferreira, I.C.F.R.; et al. Evaluation of the Phenolic Profile of Castanea sativa Mill. By-Products and Their Antioxidant and Antimicrobial Activity against Multiresistant Bacteria. *Antioxidants* **2020**, *9*, 87. [CrossRef]
9. Corregidor, V.; Antonio, A.L.; Alves, L.C.; Cabo Verde, S. Castanea sativa shells and fruits: Compositional analysis by proton induced X-ray emission. *Nucl. Instrum. Methods Phys. Res. Sect. B Beam Interact. Mater. Atoms* **2020**, *477*, 98–103. [CrossRef]
10. Neves, J.M.; Matos, C.; Moutinho, C.; Queiroz, G.; Gomes, L.R. Ethnopharmacological notes about ancient uses of medicinal plants in Trás-os-Montes (northern of Portugal). *J. Ethnopharmacol.* **2009**, *124*, 270–283. [CrossRef] [PubMed]
11. Comandini, P.; Lerma-García, M.J.; Simó-Alfonso, E.F.; Toschi, T.G. Tannin analysis of chestnut bark samples (*Castanea sativa* Mill.) by HPLC-DAD–MS. *Food Chem.* **2014**, *157*, 290–295. [CrossRef] [PubMed]
12. de Vasconcelos, M.C.B.M.; Bennett, R.N.; Rosa, E.A.S.; Ferreira-Cardoso, J.V. Composition of European chestnut (Castanea sativa Mill.) and association with health effects: Fresh and processed products. *J. Sci. Food Agric.* **2010**, *90*, 1578–1589. [CrossRef] [PubMed]
13. Ozkan, G.; Günal-Köroğlu, D.; Capanoglu, E. Valorization of fruit and vegetable processing by-products/wastes. *Adv. Food Nutr. Res.* **2023**, *107*, 1–39. [CrossRef] [PubMed]
14. Santos, M.J.; Pinto, T.; Vilela, A. Sweet Chestnut (*Castanea sativa* Mill.) Nutritional and Phenolic Composition Interactions with Chestnut Flavor Physiology. *Foods* **2022**, *11*, 4052. [CrossRef] [PubMed]
15. Fernandes, P.; Colavolpe, M.B.; Serrazina, S.; Costa, R.L. European and American chestnuts: An overview of the main threats and control efforts. *Front. Plant Sci.* **2022**, *13*, 951844. [CrossRef] [PubMed]
16. Hu, W.; Zhang, X.; Chen, M.; Rahman, S.T.; Li, X.; Wang, G. Enhancing Cr (VI) Adsorption of Chestnut Shell Biochar through H3PO4 Activation and Nickel Doping. *Molecules* **2024**, *29*, 2220. [CrossRef] [PubMed]
17. Sangiovanni, E.; Piazza, S.; Vrhovsek, U.; Fumagalli, M.; Khalilpour, S.; Masuero, D.; Di Lorenzo, C.; Colombo, L.; Mattivi, F.; De Fabiani, E.; et al. A bio-guided approach for the development of a chestnut-based proanthocyanidin-enriched nutraceutical with potential anti-gastritis properties. *Pharmacol. Res.* **2018**, *134*, 145–155. [CrossRef] [PubMed]
18. Weiner, L.M.; Webb, A.K.; Limbago, B.; Dudeck, M.A.; Patel, J.; Kallen, A.J.; Edwards, J.R.; Sievert, D.M. Antimicrobial-Resistant Pathogens Associated with Healthcare-Associated Infections: Summary of Data Reported to the National Healthcare Safety Network at the Centers for Disease Control and Prevention, 2011–2014. *Infect. Control Hosp. Epidemiol.* **2016**, *37*, 1288–1301. [CrossRef] [PubMed]
19. Baddour, L.M.; Wilson, W.R.; Bayer, A.S.; Fowler, V.G.; Bolger, A.F.; Levison, M.E.; Ferrieri, P.; Gerber, M.A.; Tani, L.Y.; Gewitz, M.H.; et al. Infective endocarditis: Diagnosis, antimicrobial therapy, and management of complications: A statement for healthcare professionals from the Committee on Rheumatic Fever, Endocarditis, and Kawasaki Disease, Council on Cardiovascular Disease in the Young, and the Councils on Clinical Cardiology, Stroke, and Cardiovascular Surgery and Anesthesia, American Heart Association: Endorsed by the Infectious Diseases Society of America. *Circulation* **2005**, *111*, e394–e434. [CrossRef] [PubMed]
20. Murray, B.E. The life and times of the Enterococcus. *Clin. Microbiol. Rev.* **1990**, *3*, 46. [CrossRef]
21. Hollenbeck, B.L.; Rice, L.B. Intrinsic and acquired resistance mechanisms in enterococcus. *Virulence* **2012**, *3*, 421. [CrossRef]
22. Trezza, A.; Geminiani, M.; Cutrera, G.; Dreassi, E.; Frusciante, L.; Lamponi, S.; Spiga, O.; Santucci, A. A Drug Discovery Approach to a Reveal Novel Antioxidant Natural Source: The Case of Chestnut Burr Biomass. *Int. J. Mol. Sci.* **2024**, *25*, 2517. [CrossRef] [PubMed]

23. Johnson, M.; Zaretskaya, I.; Raytselis, Y.; Merezhuk, Y.; McGinnis, S.; Madden, T.L. NCBI BLAST: A better web interface. *Nucleic Acids Res.* **2008**, *36*, W5–W9. [CrossRef] [PubMed]
24. UniProt Consortium. UniProt: The Universal Protein Knowledgebase in 2023. *Nucleic Acids Res.* **2023**, *51*, D523–D531. [CrossRef] [PubMed]
25. Jumper, J.; Evans, R.; Pritzel, A.; Green, T.; Figurnov, M.; Ronneberger, O.; Tunyasuvunakool, K.; Bates, R.; Žídek, A.; Potapenko, A.; et al. Highly accurate protein structure prediction with AlphaFold. *Nature* **2021**, *596*, 583–589. [CrossRef] [PubMed]
26. Kant, A.; Palva, A.; von Ossowski, I.; Krishnan, V. Crystal structure of lactobacillar SpaC reveals an atypical five-domain pilus tip adhesin: Exposing its substrate-binding and assembly in SpaCBA pili. *J. Struct. Biol.* **2020**, *211*, 107571. [CrossRef] [PubMed]
27. Janson, G.; Paiardini, A. PyMod 3: A complete suite for structural bioinformatics in PyMOL. *Bioinformatics* **2021**, *37*, 1471–1472. [CrossRef]
28. Laskowski, R.A.; Rullmannn, J.A.; MacArthur, M.W.; Kaptein, R.; Thornton, J.M. AQUA and PROCHECK-NMR: Programs for checking the quality of protein structures solved by NMR*. *J. Biomol. NMR* **1996**, *8*, 477–486. [CrossRef] [PubMed]
29. Jo, S.; Kim, T.; Iyer, V.G.; Im, W. CHARMM-GUI: A web-based graphical user interface for CHARMM. *J. Comput. Chem.* **2008**, *29*, 1859–1865. [CrossRef] [PubMed]
30. Abraham, M.J.; Murtola, T.; Schulz, R.; Páll, S.; Smith, J.C.; Hess, B.; Lindah, E. GROMACS: High performance molecular simulations through multi-level parallelism from laptops to supercomputers. *SoftwareX* **2015**, *1–2*, 19–25. [CrossRef]
31. Trezza, A.; Birgauan, A.; Geminiani, M.; Visibelli, A.; Santucci, A. Molecular and Evolution In Silico Studies Unlock the h4-HPPD C-Terminal Tail Gating Mechanism. *Biomedicines* **2024**, *12*, 1196. [CrossRef]
32. Trezza, A.; Spiga, O.; Mugnai, P.; Saponara, S.; Sgaragli, G.; Fusi, F. Functional, electrophysiology, and molecular dynamics analysis of quercetin-induced contraction of rat vascular musculature. *Eur. J. Pharmacol.* **2022**, *918*, 174778. [CrossRef]
33. Carullo, G.; Ahmed, A.; Trezza, A.; Spiga, O.; Brizzi, A.; Saponara, S.; Fusi, F.; Aiello, F. A multitarget semi-synthetic derivative of the flavonoid morin with improved in vitro vasorelaxant activity: Role of CaV1.2 and KCa1.1 channels. *Biochem. Pharmacol.* **2021**, *185*, 114429. [CrossRef]
34. Sayers, E.W.; Bolton, E.E.; Brister, J.R.; Canese, K.; Chan, J.; Comeau, D.C.; Connor, R.; Funk, K.; Kelly, C.; Kim, S.; et al. Database resources of the national center for biotechnology information. *Nucleic Acids Res.* **2022**, *50*, D20–D26. [CrossRef]
35. Rosignoli, S.; Paiardini, A. DockingPie: A consensus docking plugin for PyMOL. *Bioinformatics* **2022**, *38*, 4233–4234. [CrossRef]
36. Trott, O.; Olson, A.J. AutoDock Vina: Improving the speed and accuracy of docking with a new scoring function, efficient optimization and multithreading. *J. Comput. Chem.* **2010**, *31*, 455–461. [CrossRef]
37. Fusi, F.; Durante, M.; Spiga, O.; Trezza, A.; Frosini, M.; Floriddia, E.; Teodori, E.; Dei, S.; Saponara, S. In vitro and in silico analysis of the vascular effects of asymmetrical N,N-bis(alkanol)amine aryl esters, novel multidrug resistance-reverting agents. *Naunyn-Schmiedeberg's Arch. Pharmacol.* **2016**, *389*, 1033–1043. [CrossRef]
38. Salentin, S.; Schreiber, S.; Haupt, V.J.; Adasme, M.F.; Schroeder, M. PLIP: Fully automated protein–ligand interaction profiler. *Nucleic Acids Res.* **2015**, *43*, W443. [CrossRef]
39. Fusi, F.; Trezza, A.; Spiga, O.; Sgaragli, G.; Bova, S. Cav1.2 channel current block by the PKA inhibitor H-89 in rat tail artery myocytes via a PKA-independent mechanism: Electrophysiological, functional, and molecular docking studies. *Biochem. Pharmacol.* **2017**, *140*, 53–63. [CrossRef]
40. Thompson, J.D.; Higgins, D.G.; Gibson, T.J. CLUSTAL W: Improving the sensitivity of progressive multiple sequence alignment through sequence weighting, position-specific gap penalties and weight matrix choice. *Nucleic Acids Res.* **1994**, *22*, 4673–4680. [CrossRef]
41. Salam, M.A.; Al-Amin, M.Y.; Salam, M.T.; Pawar, J.S.; Akhter, N.; Rabaan, A.A.; Alqumber, M.A.A. Antimicrobial Resistance: A Growing Serious Threat for Global Public Health. *Healthcare* **2023**, *11*, 1946. [CrossRef]
42. Bueno-Gavilá, E.; Abellán, A.; Girón-Rodríguez, F.; Cayuela, J.M.; Salazar, E.; Gómez, R.; Tejada, L. Bioactivity of hydrolysates obtained from bovine casein using artichoke (*Cynara scolymus* L.) proteases. *J. Dairy Sci.* **2019**, *102*, 10711–10723. [CrossRef] [PubMed]
43. Ciríaco, M.; Patarata, L.; Moura-Alves, M.; Nunes, F.; Saraiva, C. Antimicrobial Properties of Chestnut Shell Extract as an Ecofriendly Approach for Food Preservation. *Biol. Life Sci. Forum* **2023**, *26*, 123. [CrossRef]
44. Štumpf, S.; Hostnik, G.; Langerholc, T.; Pintarič, M.; Kolenc, Z.; Bren, U. The Influence of Chestnut Extract and Its Components on Antibacterial Activity against Staphylococcus aureus. *Plants* **2023**, *12*, 2043. [CrossRef] [PubMed]
45. Frusciante, L.; Geminiani, M.; Olmastroni, T.; Mastroeni, P.; Trezza, A.; Salvini, L.; Lamponi, S.; Spiga, O.; Santucci, A. Repurposing Castanea sativa Spiny Burr By-Products Extract as a Potentially Effective Anti-Inflammatory Agent for Novel Future Biotechnological Applications. *Life* **2024**, *14*, 763. [CrossRef]